Local boron environment in Ni_{100-x} B_x metallic glasses: An NMR study

P. Panissod and I. Bakonyi*

Laboratoire de Magnetisme et de Structure Electronique des Solides (Laboratoire No. 306 associé au Centre National de la Recherche Scientifique), Institut Le Bel, Université Louis Pasteur, 4 rue Blaise Pascal, F-67070 Strasbourg Cedex, France.

R. Hasegawa

Corporate Research and Development Center, Allied Corporation, P.O. Box 1021R, Morristown, New Jersey 07960

From the analysis of the ^{11}B NMR spectra in a-$Ni_{100-x}B_x$ ($18.5 \leq x \leq 40$) the electric-field-gradient (EFG) components on the B sites and their distributions are deduced, giving an insight into the local atomic arrangements. For $x = 18.5$ and 40, one finds relatively narrow distributions of the EFG components, indicating weak fluctuations of the bonding angles, distances, and nature of the atoms in the B coordination shell. The comparison with the compositionally closest nickel borides (Ni_3B and Ni_4B_3) immediately suggests that the local structure around B is similar in these glasses and in the related crystals, i.e., nickel trigonal prisms (6 Ni) whose rectangular faces are capped by 3 Ni (Ni_3B) or 3 Ni and/or B (Ni_4B_3). For intermediate concentrations the EFG component distributions are found significantly broader and comparable with those expected from random packing of spheres. However, the continuous evolution of the NMR spectra shape with increasing B content rather suggests an admixture of c-Ni_3B—like and c-Ni_4B_3—like B local environment; i.e., when B concentration increases, more prisms share rectangular faces allowing boron-boron contact as in c-Ni_4B_3. No sign of a B coordination shell similar to that in c-Ni_2B (8 Ni anticubes + 2 B) is found in the glasses. Measurements of transverse relaxation times T_2, which reflect essentially the B—B bondings, qualitatively support these conclusions.

I. INTRODUCTION

Studies of the crystal-field parameters in amorphous materials have proved useful for the understanding of the amorphous structure[1,2] as they give information on the symmetry properties of the local structure while usual spectroscopic techniques essentially give information about distances. NMR has been widely used for that purpose in insulating glasses.[3] For amorphous metals a previous NMR study in a-$La_{75}Ga_{25}$, a-$Mo_{70}B_{30}$, and a-$Ni_{78}P_{14}B_8$ has shown that their structure retains to a significant extent the local symmetry around the glass former prevailing in the corresponding crystalline materials (c-La_3Ga, cubic; c-Mo_2B, uniaxial; c-Ni_3B, nonuniaxial).[4]

The present study has been performed in two-component metal-metalloid glasses, i.e., a-$Ni_{100-x}B_x$ for an extended concentration range ($18.5 \leq x \leq 40$) which includes compositions close to the crystalline nickel borides: c-Ni_3B, c-Ni_2B, and c-Ni_4B_3. The obvious purpose of this work was to study the modifications of the amorphous structure with varying metalloid concentration and to compare it with that of the crystalline counterparts.

Most of the information on the amorphous structure was obtained in this work through the study of quadrupolar interactions between the nuclear quadrupole moment of ^{11}B ($I = \frac{3}{2}$) and the local electric field gradient (EFG) whose symmetry reflects that of the local environment of the probe nucleus. The traceless EFG tensor is determined by the quadrupolar frequency $\nu_Q = 3e^2qQ/2I(2I+1)\hbar$ (proportional to its largest eigenvalue $eq = V_{zz}$) and by a dimensionless coefficient $\eta = |V_{xx} - V_{yy}| / |V_{zz}|$.

The asymmetry parameter η is a measure of the deviation from an uniaxial local symmetry (which for $\eta = 0$) and ν_Q is a measure of the deviation from cubic symmetry (which for $V_{xx} = V_{yy} = V_{zz} = 0$). As shown in Fig. 1, the NMR spectrum shape is very sensitive to ν_Q and η and these values can usually be obtained directly from the spectrum in crystalline materials. In amorphous materials fluctua-
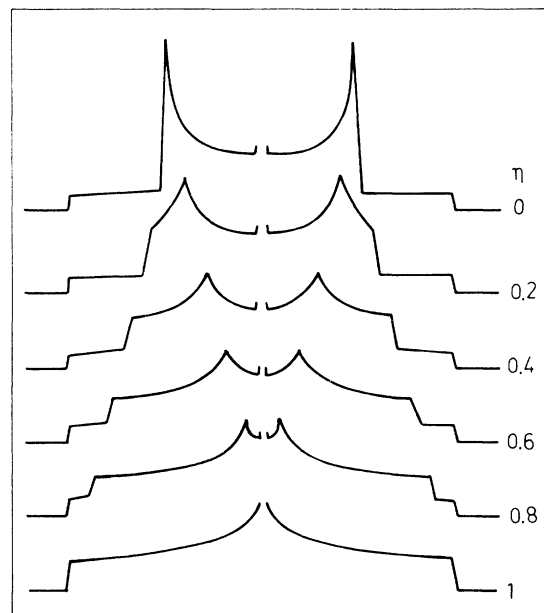

FIG. 1. Unbroadened NMR "powder" spectra for η varying from 0 to 1.

tions of the local environment from site to site rather smear off the details of the spectrum and although the local symmetry of the EFG (cubiclike, uniaxial, or nonuniaxial) can be qualitatively deduced directly, computer fits are needed for quantitative comparisons.

Some more information was obtained through the measurement of the transverse relaxation time T_2 which is dominated by B nuclei spin-spin interactions and hence related mostly to B—B bondings. As a major conclusion, this study shows that B atoms in a-$Ni_{100-x}B_x$ glasses are most probably surrounded by nickel trigonal prisms as in c-Ni_3B and c-Ni_4B_3 (orthorhombic); the increase of the B concentration would be accommodated by changes in the packing of the prisms allowing more B—B bondings.

II. SAMPLE PREPARATION AND EXPERIMENT

a-$Ni_{100-x}B_x$ samples were prepared by rapid quenching (melt spinning). They could be obtained amorphous (as checked by x-ray diffraction) around $x = 18.5$ (eutectic composition), $x = 25$, and on a broader concentration range from $x = 31$ (second eutectic) to $x = 40$. Samples with high B content are rather brittle; this was previously mentioned by Donald and Davies[5] and attributed to directional B—B covalent bondings.

Crystalline samples were prepared by sintering of the elements in a sealed quartz tube; for c-Ni_4B_3 there exist two allotropic varieties, one orthorhombic on the low-B side and one monoclinic on the high-B-content side. The former one was synthetized for comparison purpose since amorphous samples have lower B content than 43 at. %.

NMR spectra of the ^{11}B nucleus ($I = \frac{3}{2}$) were observed on a conventional pulsed NMR spectrometer at $\nu = 16.592$ MHz. They were obtained from integral spin echo intensity versus external field. T_2 was measured conventionally through the decay of the spin echo intensity versus delay between $\pi/2 - \pi$ pulses. Measurements were carried out at 4.2 K except for a-$Ni_{81.5}B_{18.5}$ which for the strong magnetic broadening at low temperatures precluded accurate observations.

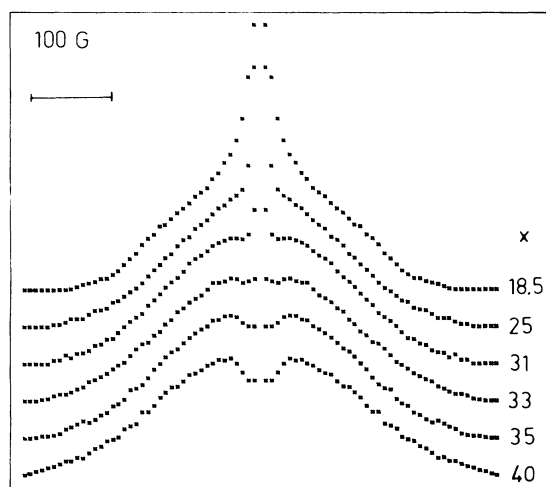FIG. 3. Experimental NMR spectra in c-Ni_3B, c-Ni_2B, and c-Ni_4B_3 (orthorhombic) (Ref. 11).

III. RESULTS AND ANALYSIS

A. Spectra and EFG parameters

The experimental spectra presented in Fig. 2 (glasses) and Fig. 3 (crystalline compounds) indicate obvious similarities between the EFG's around boron in the glasses for

FIG. 2. Experimental NMR spectra in a-$Ni_{100-x}B_x$ samples. All spectra $T = 4.2$ K except $x = 18.5$ (100 K) (Ref. 11).

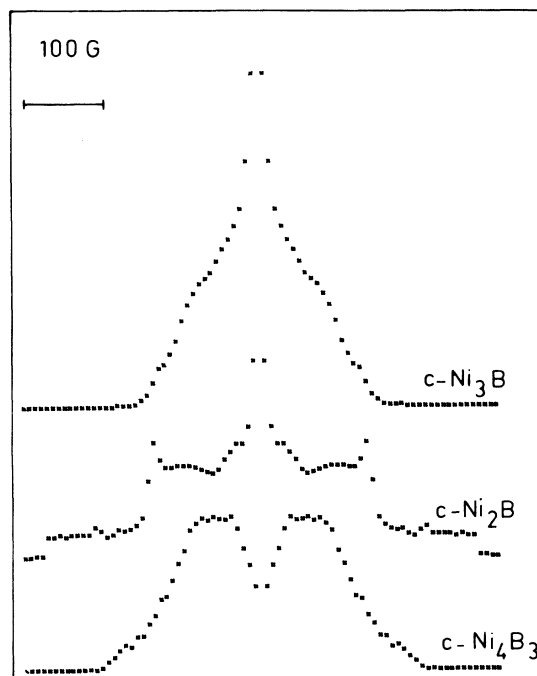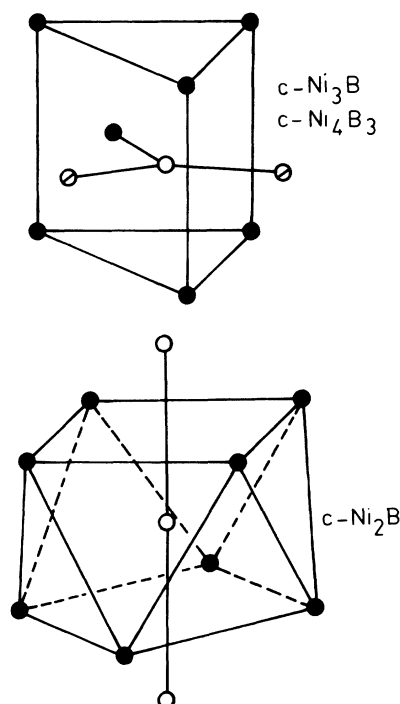FIG. 4. Boron coordination shell in c-Ni_2B and c-Ni_3B or c-Ni_4B_3. O, B; ●, Ni; ◐, Ni (in c-Ni_3B or for B_{III} in c-Ni_4B_3), B_I or B_{II} (for B_I or B_{II}, respectively, in c-Ni_4B_3).

$x = 18.5$ and 40 and those in c-Ni$_3$B and c-Ni$_4$B$_3$, respectively. But the uniaxial symmetry of the EFG in c-Ni$_2$B is not found in the amorphous modification and rather a continuous evolution of the spectra shape is observed with increasing B content. This observation indicates that the average boron local environment changes progressively in the glasses while in the crystalline compounds the B coordination shell is quite different in c-Ni$_2$B [anticubes of (8 Ni + 2 B) in a tetragonal I_4/mcm structure] and in c-Ni$_3$B (trigonal prisms of 6 Ni and 3 Ni at pyramid apexes in an orthorhombic $Pnma$ structure) or in c-Ni$_4$B$_3$ (trigonal prisms of 6 Ni and 3 Ni or B at pyramid apexes in $Pnma$ structure) (Fig. 4). These qualitative remarks suggest that the boron coordination in the glasses could closely resemble that of B in c-Ni$_3$B for the low-B concentration and that of B in c-Ni$_4$B$_3$ for the high B content and interpolates between them for intermediate concentrations.

More quantitative informations about the EFG parameters are obtained through computer simulation of the experimental spectra. The relevant parameters for the fit are the EFG reduced component ($\bar{v}_Q$ and η) and, for the amorphous samples, the rms half-width σ of the distribution of the EFG strength v_Q (or the more convenient ratio $\sigma/\bar{v}_Q$ which measures the degree of disorder). Although the asymmetry parameter η certainly fluctuates from site to site in the glasses, no significant improvement of the fits is observed using distributions of η and the shape of the simulated spectra is found to be very insensitive to that distribution except for very broad ones. Thus no systematic attempt to introduce such distribution was made but experimental spectra were compared with the one that would result from the broad distributions of v_Q and η computed for random packed networks (RPN) of spheres by Czjzek[1] (one size) and Takacs (two sizes plus metalloid-metalloid avoidance),[6] both computations giving very similar distributions shapes. A reason for the weak influence of η distribution on the spectrum shape may be due to the fact that a nonzero η value already implies a distribution of EFG strength in the plane perpendicular to its principal axis; indeed η and $\sigma/\bar{v}_Q$ are found interdependent in the fits in the sense that constraining η to a higher value reduces the computed $\sigma/\bar{v}_Q$ and vice versa. We shall first present the results for the crystalline compounds, then for the glasses with $x = 18.5$ and 40 of which analysis is rather unambiguous and finally for the glasses with intermediate concentrations.

Crystalline nickel borides. The value for v_Q and η in these compounds are presented in Table I. In c-Ni$_3$B and c-Ni$_2$B, these values are obtained directly from the spectra.

TABLE I. EFG parameters around B in crystalline nickel borides.

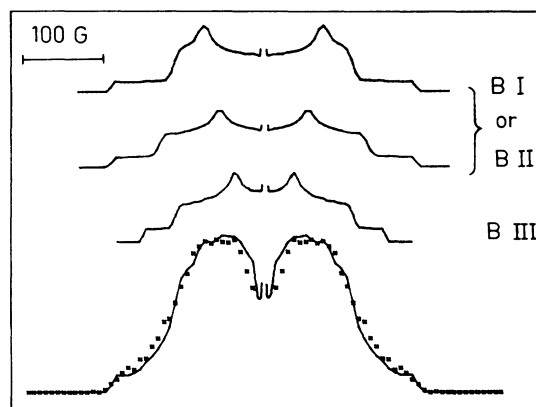| Compound		v_Q (kHz)	η
c-Ni$_3$B		180 ± 10	0.6 ± 0.05
c-Ni$_2$B		360 ± 10	0
c-Ni$_4$B$_3$	B$_I$		0.2 ± 0.1
	or	230 ± 20	
	B$_{II}$		0.4 ± 0.1
(ortho)	B$_{III}$	190 ± 30	0.5 ± 0.1

FIG. 5. B$_I$, B$_{II}$, and B$_{III}$ NMR subspectra as obtained by fit of the B NMR spectrum in c-Ni$_4$B$_3$.

For c-Ni$_4$B$_3$ the situation is more complex due to the presence of three different crystallographic B sites and we had to use computer simulation to determine the six different EFG parameters as described below. First, the highest value for v_Q is obtained from the overall width of the spectrum; from the step heights at both ends of the spectra it was deduced that this highest v_Q corresponds to two sites among the three different ones. These results are independent of the values for η's. Then from the examination of the boron coordination shell for the three sites it was presumed that the third site corresponds to B with no B nearest neighbors B$_{III}$. Indeed it is highly probable that the highest v_Q value corresponds to the two sites with two B nearest neighbors (B$_I$ and B$_{II}$), a situation being similar to that of B in c-Ni$_2$B; a calculation of the EFG in a point-charge model (PCM) supports this assumption since it yields comparable v_Q's for B$_I$ and B$_{II}$ and a much lower v_Q for B$_{III}$ emphasizing the role of the two B nearest neighbors. Trial values of η's on B$_I$ and B$_{II}$ sites were
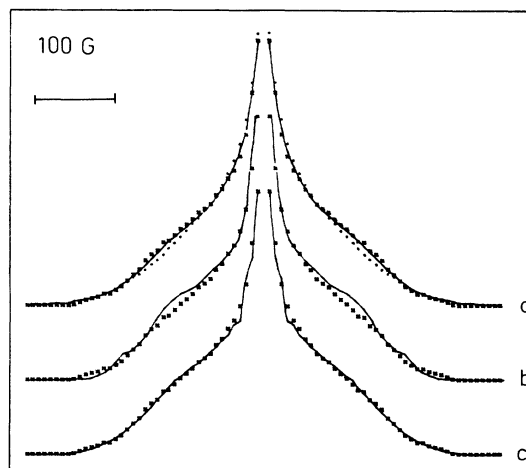

FIG. 6. B experimental NMR spectrum in a-Ni$_{81.5}$B$_{18.5}$ (crosses). Curve a, simulated spectrum for $\bar{v}_Q = 230$ kHz, $\eta = 0.6$, $\sigma/\bar{v}_q = 0.15$ (fit includes Lorentzian magnetic broadening). (Dots: same except $\sigma/\bar{v}_Q = 0.25$.) Curve b, B experimental spectrum in c-Ni$_3$B expanded 35% along the horizontal axis. Curve c, same as b except a 15% rms width distribution of the expansion factor is added.

consecutively obtained by a first fit assuming that ν_Q and η on B_{III} are the same as in c-Ni_3B (same environment). The values for η and ν_Q on B_{III} and η's on B_I and B_{II} were obtained in the final refinement (Fig. 5).

a-$Ni_{81.5}B_{18.5}$. For this sample, a significant overall Lorentzian broadening had to be introduced to reproduce the central line width [HWHM (half-width at half maximum) $=15$ G]; this broadening results from magnetic homogeneities in the sample probably due to precipitation of small nickel particles (about 3% of the total volume).[7] Then an excellent fit of the spectrum is obtained for $\bar{\nu}_Q=230\pm10$ kHz, $\eta=0.6\pm0.1$, and $\sigma/\bar{\nu}_Q\lesssim0.15$ (Fig. 6). Comparable values were obtained previously[4] for B in a-$Ni_{78}P_{14}B_8$ (220 ± 20 kHz, 0.65 ± 0.15, and 0.25 ± 0.05 for $\bar{\nu}_Q$, η, and $\sigma/\bar{\nu}_Q$); however, the degree of disorder $\sigma/\bar{\nu}_Q$ is slightly higher in this last sample certainly because of chemical disorder introduced by the presence of two metalloids. The comparison with c-Ni_3B shows that the symmetry of the EFG on B sites is the same in the crystalline and the glassy compounds ($\eta=0.6$). The strength of the EFG is however 30—40% higher in the glass. Indeed the spectrum in c-Ni_3B compares quite well with that in a-$Ni_{81.5}B_{18.5}$ once expanded 35% horizontally to take into account the higher $\bar{\nu}_Q$; once added a distribution of the expansion factor (to simulate the distribution of ν_Q's) both spectra can be superimposed; this obviously confirms the direct fit. Furthermore, one should note that these results are not consistent with random packed structure calculations: Firstly, $\sigma/\bar{\nu}_Q$ is much lower than the value predicted for RPN [$\sigma/\bar{\nu}_Q\simeq0.3$ for spheres of equal radius to $\sigma/\bar{\nu}_Q\simeq0.5$ for an atomic radii ratio r(metal)—r(metalloid) equal to 1.4, which is our case], and secondly, the relatively sharp decrease of the signal at both ends of the spectrum which results from high but weakly fluctuating η cannot be observed for a RPN.

a-$Ni_{60}B_{40}$. For this sample a good fit was obtained for $\bar{\nu}_Q=300\pm30$ kHz, $\eta=0.4\pm0.1$, and $\sigma/\bar{\nu}_Q=0.25$ (Fig. 7). The lower value for η could be predicted from the dips close to the central peak which are not compatible with the distribution of η's computed in a random packed network. These values again compare well with those found in c-Ni_4B_3 ($\bar{\nu}_Q=230$ kHz, $\bar{\eta}=0.37$) although again $\bar{\nu}_Q$ is 30—40% higher in the glass than in the crystal. The
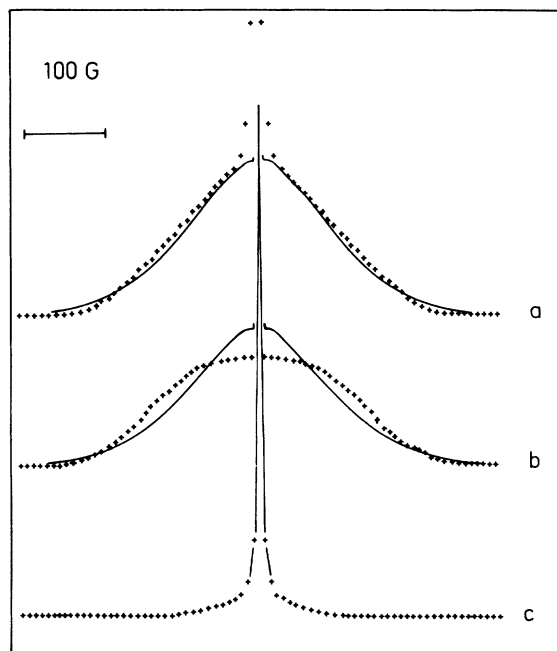
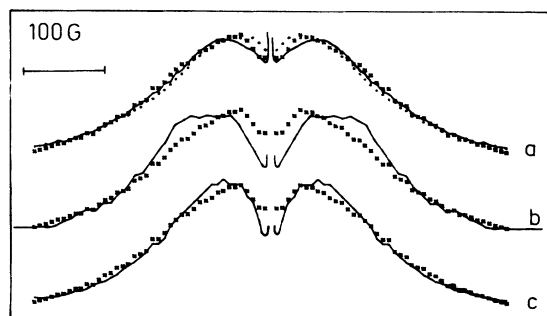FIG. 8. Curve a, B experimental NMR spectrum in a-$Ni_{75}B_{25}$ (crosses). Full line: spectrum simulated with the $\bar{\nu}_Q$ and η distributions computed for a random packed network (no other broadening added). Curve b, same as above except the central line ($\frac{1}{2}\leftrightarrow-\frac{1}{2}$ transition) is experimentally reduced 10 times with respect to the quadrupole wings ($\pm\frac{3}{2}\leftrightarrow\pm\frac{1}{2}$ transitions) (see text). Curve c, central line shape deduced by subtracting b from a (reduced 2.5 times with respect to a and b).

value for σ/ν_Q is also slightly higher than in a-$Ni_{81.5}B_{18.5}$ but one should note that ν_Q also fluctuates from site to site in c-Ni_4B_3 ($\sigma/\bar{\nu}_Q=0.1$). The quality of the fit could obviously be improved using distributions around several $\bar{\nu}_Q$ but this would give ambiguous results owing to the number of independent parameters. Therefore, a direct comparison with the spectrum in c-Ni_4B_3 has also been performed: As shown in Fig. 7 the spectrum of B in a-$Ni_{60}B_{40}$ can be reproduced nearly exactly with the expanded and broadened spectrum of B in c-Ni_4B_3. Although the spectra do not compare as perfectly as for a-$Ni_{81.5}B_{18.5}$ and c-Ni_3B one can see that the agreement could be further improved if one assumes that B with no B nearest neighbors (c-Ni_3B—like or B_{III}) are more numerous in the glass than in the crystal which is consistent with the lower B content in the glass.

Intermediate concentrations. For $x=25$, although this sample corresponds exactly to c-Ni_3B the spectrum shape already deviates more from the crystalline case than in a-$Ni_{81.5}B_{18.5}$ and simulations show a higher disorder ($\sigma/\bar{\nu}_Q\simeq0.3$). For $x=33$, the spectrum shape cannot be related in any way to that for c-Ni_2B: Simulations show high nonuniaxiality ($\eta\simeq0.5$) and also high disorder.

The spectra for $x=25,31,33$ are the closest to the one that would result from random packing. Indeed an agreement is found between the shapes of the spectrum for $x=25$ and the spectrum computed for a RPN if the dipolar broadening of the central line is not taken into account in the fit. This agreement, however, is fortuitous: Taking advantage of the shorter T_2 on the central line than on the

FIG. 7. B experimental NMR spectrum in a-$Ni_{60}B_{40}$ (crosses). Curve a, simulated spectrum for $\bar{\nu}_Q=300$ kHz, $\eta=0.4$, $\sigma/\bar{\nu}_Q=0.25$. (Dots: same except $\sigma/\bar{\nu}_Q=0.3$.) Curve b, B experimental spectrum in c-Ni_4B_3 expanded 35% along the horizontal axis. Curve c, same as b except a 25% rms width distribution of the expansion factor is added.

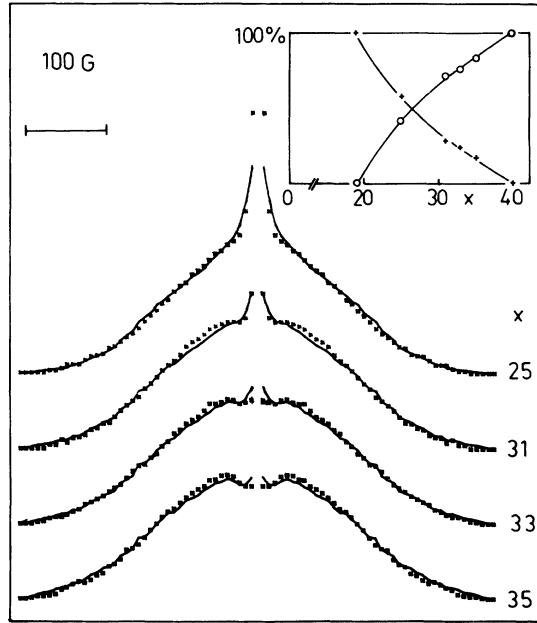P. PANISSOD, I. BAKONYI, AND R. HASEGAWA

FIG. 9. Fit of the spectra in a-$Ni_{100-x}B_x$ ($25 \leq x \leq 35$) with a weighted sum of spectra observed in a-$Ni_{81.5}B_{18.5}$ and a-$Ni_{60}B_{40}$. Inset: relative intensities of the a-$Ni_{81.5}B_{18.5}$ ($+$) and a-$Ni_{60}B_{40}$ ($\bigcirc$) spectra as function of B content.

quadrupolar wings (see next section) one can strongly reduce the contribution to the spectrum of the central line ($\frac{1}{2} \rightarrow -\frac{1}{2}$ transition). In such a case one sees that the spectrum corresponding to the $\pm\frac{3}{2} \leftrightarrow \pm\frac{1}{2}$ transitions is much flatter close to the center and the misfit with the RPN spectrum is more evident (Fig. 8).

Actually, as mentioned before, the spectrum shape changes progressively with increasing B content and dips on each side of the central line become apparent for $x = 33$ and evident for $x = 35$, indicating a reduction of the average η from 0.6 ($x = 18.5$) to 0.4 ($x = 40$). Indeed an excellent fit of the spectra for $25 \leq x \leq 35$ can be obtained with a weighted sum of the spectra for $x = 18.5$ and 40 (Fig. 9).

B. Tranverse—relaxation-time measurements

In the nickel borides owing to the very low nuclear moment of Ni and the very long spin-lattice relaxation times,

the transverse relaxation T_2 reflects essentially the spin-spin interaction between B nuclei. Hence this measurement can give an insight into the boron-boron distances and arrangements. Since B nuclei experience quadrupole interaction, T_2 has been measured on the central line ($\frac{1}{2} \leftrightarrow -\frac{1}{2}$ transition: T_{2c}) and on the quadrupolar wings ($\pm\frac{3}{2} \leftrightarrow -\pm\frac{1}{2}$ transition: T_{2w}). For all samples the transverse nuclear magnetization decay was found exponential (except perhaps for very short times $\tau < 50$ μs). This means that the dipolar line broadening results in a (truncated) Lorentzian-type shape which is clearly observed in c-Ni_2B (broad foot of the central line, Fig. 3) or in a-$Ni_{75}B_{25}$ (Fig. 8) and explains why the peaks close to the central line for $\eta = 0.6$ are not resolved in c-Ni_3B. Thus T_2's are well defined and the results are summarized in Table II. Because of the Lorentzian-type shape, T_2 is a measure of the inverse HWHM which can hardly be related to the rms half-width of the dipolar broadening unless the fourth moment of the dipolar broadening could be computed. This is totally unachievable in such complex structures for powder samples and with quadrupolar interaction. Unfortunately the HWHM is much less sensitive to the distribution of distances than the rms width (or the second moment). However, qualitative conclusions can be drawn from the comparison between glasses and crystals.

First, as shown on Table II, T_{2c} scales with the cube of the average B-B distance in crystalline materials and also with the inverse boron concentration in all samples. This shows that the average B-B distances are the same in the glasses and in the crystal of same composition.

Second, T_{2w} is usually much longer than T_{2c} except in c-Ni_2B. This is qualitatively understood in the following way: In c-Ni_2B all boron spins are like-spins, i.e., the central B atom and all its B neighbors experience the same EFG (strength and orientation); thus the three different frequencies for the three transitions are the same for the central nucleus and for its neighbors resulting in an efficient dipolar coupling whatever transition is concerned. On the contrary, only part of the B spins in the neighborhood of the central atom are like spins in c-Ni_3B and none in c-Ni_4B_3; others are unlike spins experiencing EFG with different orientation (Ni_3B) and/or different strength (Ni_4B_3). This reduces much more the dipolar transition

TABLE II. Transverse relaxation times in crystalline and glassy nickel borides (T_{2c}, central line; T_{2w}, quadrupolar wings), $\langle r_{B-B} \rangle$, average boron-boron distance, and x, boron concentration.

Compound	T_{2c} (μs)	T_{2w} (μs)	$T_{2c}/\langle r_{B-B} \rangle^3$ (μs/Å^{+3})	$(x/100)T_{2c}$ (μs)	T_{2c}/T_{2w}
c-Ni_3B	580 ± 50	890 ± 100	15.4 ± 2	14.5	0.65
c-Ni_2B	380 ± 40	430 ± 80	14.4 ± 2	13.0	0.88
c-Ni_4B_3	330 ± 40	590 ± 100	16.9 ± 2	14.0	0.56
a-$Ni_{81.5}B_{18.5}$	800 ± 100	1800 ± 400		15.0	0.45
a-$Ni_{75}B_{25}$	540 ± 50	1410 ± 100		13.5	0.36
a-$Ni_{69}B_{31}$	515 ± 50	1270 ± 100		16.0	0.41
a-$Ni_{67}B_{33}$	425 ± 40	945 ± 100		14.0	0.45
a-$Ni_{65}B_{35}$	400 ± 40	820 ± 100		14.0	0.48
a-$Ni_{60}B_{40}$	390 ± 40	810 ± 100		16.0	0.48

probability for $\pm\frac{3}{2}\leftrightarrow\pm\frac{1}{2}$ transitions than for $\frac{1}{2}\leftrightarrow-\frac{1}{2}$ transition whose frequency is, only in second order, dependent on the EFG. Hence the T_{2c}/T_{2w} ratio reported in Table II is a qualitative measure of the relative number of B nuclei experiencing the same EFG as the central atom in its neighborhood or reciprocally, a measure of the difference between the EFG on the central B atom and the average EFG on its B neighbors. Now considering this ratio for the glassy samples, one sees that T_{2c}/T_{2w} is lower than in the crystals. This is expected due to structural disorder. However, the values of this parameter are rather close for a-$Ni_{60}B_{40}$ and a-Ni_4B_3 which indicates a certain coherence of the structure extending further than the first coordination shell. For decreasing B content this ratio decreases confirming the higher disorder or the greater variety of B environments for intermediate concentrations. For $x=18.5$ it increases slightly again; though there is a great uncertainty on the value of T_{2c}/T_{2w} for this sample, this is consistent with the weaker fluctuations of the B environments.

IV. DISCUSSION

In a-$Ni_{81.5}B_{18.5}$ the narrow distribution of the measured EFG parameter shows that there are only weak fluctuations of the boron coordination (position and nature of the surrounding atoms). The measured value of the asymmetry parameter η in this glass shows that the symmetry of the local charge distributions is the same as in c-Ni_3B. Although we are aware of the fact that the EFG may not be unequivocally related to the local arrangement of the surrounding atoms, these results show that in any case B atoms are not included in a random packed network of Ni atoms and that most probably they are surrounded by the same Ni trigonal prisms as in c-Ni_3B. However, boron-boron distances are larger in the glass than in the crystal due to lower B concentration which means that such prisms would be differently interconnected and hence nickel coordination might be quite different in the two compounds. The higher EFG strength ($\bar{v}_Q$) found in the glass is probably due to medium- and long-range disorder as explained below.

In Fig. 10 is shown the EFG strength [$V_{zz}(r)$], computed in a PCM for c-Ni_3B, due to atoms inside a sphere of radius r around a central B atom. It shows that the V_{zz}

due to closer atoms (within one or two atomic distances) is on the average larger by a factor of 2 than the net $V_{zz\infty}$ due to all atoms (up to 40 Å). Although PCM does not apply quantitatively to metals, this overshoot of $V_{zz}(r)$ is presumably realistic (which is also found valid for c-Ni_2B and c-Ni_4B_3). It means that in the crystals the contribution of atoms further than a few angstroms is still important since they considerably reduce the EFG due to the closer ones. On the contrary, in the glasses, the shells of neighbors distant by a few angstroms from the central atom are certainly much more isotropic (on the average) and their contribution to the mean EFG is less important than in crystals (but they will contribute to the EFG fluctuations). As a consequence the net mean EFG in glasses should be determined mostly by the closest neighbors. Recent EFG computations[6] for random networks of metal and metalloid spheres show that $V_{zz\infty}$ is attained within a few percent for a calculation limited to $r \simeq 4$ Å while in the crystalline structure $V_{zz}(r)$ is still about 50% higher than $V_{zz\infty}$ in that range. This can explain in our case the higher $\bar{v}_Q$ found in the glasses with respect to the corresponding crystals. Similarly, for a-$Ni_{60}B_{40}$, the results show that the boron environments resemble closely those in c-Ni_4B_3. Furthermore the results for T_2's can be interpreted as a trend for the trigonal prisms to pack in a similar way as in the crystal, i.e., to share rectangular faces allowing B—B bondings which is consistent with the brittleness of the samples with the high B content.

For the intermediate concentration range ($25 \leq x \leq 35$), the situation is less clear. Actually we cannot exclude the

FIG. 11. v_Q (a) and η (b) marginal distributions computed for a random packed network [after Czjzek (Ref. 1)] (dashed line) and corresponding distributions for $x=31$ assuming a mixture of c-Ni_3B—like and c-Ni_4B_3—like environments (relative weight deduced from fit).
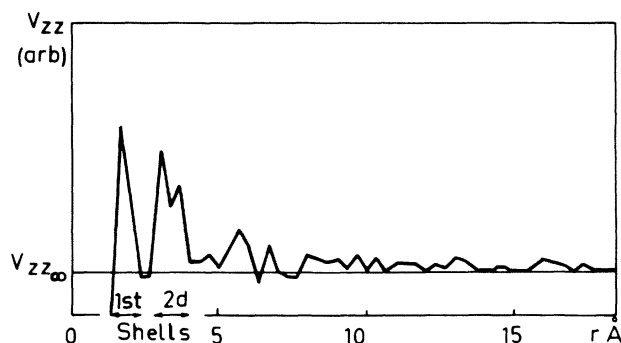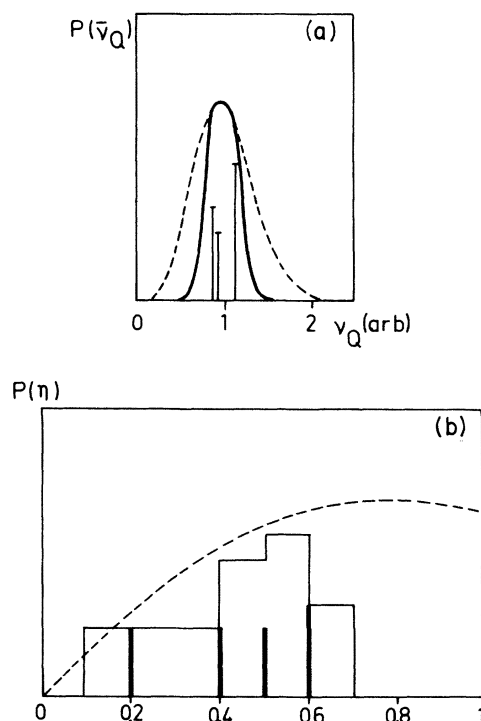
FIG. 10. V_{zz} in c-Ni_3B in a point-charge model as function of the distance from the central atom up to which the calculation is performed ($V_{zz\infty}$ computed up to 40 Å).
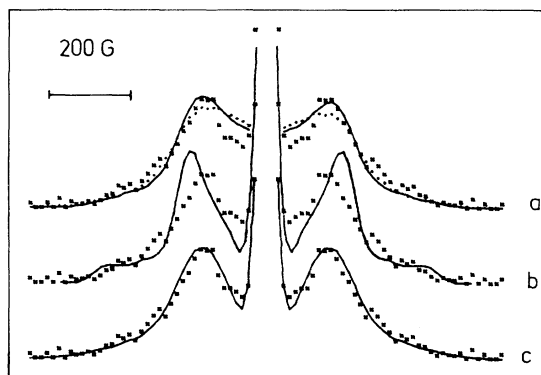
FIG. 12. B experimental spectrum in a-$Mo_{70}B_{30}$ (crosses). Curve a, simulated spectrum for $\bar{v}_Q = 420$ kHz, $\eta = 0$, $\sigma/\bar{v}_0 = 0.2$. (Dots: same except $\eta = 0$ and $\sigma > \bar{v}_Q = 0.25$ or $\eta = 0.2$ and $\sigma/\bar{v}_Q = 0.2$.) Curve b, B experimental spectrum in c-Mo_2B compressed 10% along the horizontal axis. Curve c, same as b except 20% rms width distribution of the compression factor is added.

possibility of random packed structures, particularly around $x = 31$. But the distribution of v_Q's is still narrower than that for a RPN and in our opinion the higher degree of disorder in these samples results from a mixture of c-Ni_3B—like $(a$-$Ni_{81.5}B_{18.5})$ and c-Ni_4B_3—like $(a$-$Ni_{60}B_{40})$ structures at the atomic scale. Indeed this would result in $\bar{v}_Q$'s ranging from 200 to 300 kHz and η's from 0.2 to 0.6. This gives a η distribution comparable to that computed for a RPN (Fig. 11) *except* the absence of high η's which results in spectra slightly flatter close to the central line than that for the RPN. However, this description of the glass structure in terms of c-Ni_3B—like basic cells would imply that boron atoms have no B or two B nearest neighbors only, in which case sites with two boron neighbors would form long coherent zigzag chains. Though the present experiments suggest a tendency to such coherence in a-$Ni_{60}B_{40}$, it is certain that such chains are quite limited in lengths, and that there are also sites with only one B neighbor (i.e., pairs of Ni prisms sharing 4 Ni), nonexistent in the crystalline structures.

Finally no sign of an axial boron environment similar to the Ni anticubes in c-Ni_2B is observed in the glasses. Actually it has been found[8] that one crystallization product of the amorphous samples is a metastable Ni_7B_3 phase $(x = 30)$ in which B is again at the center of Ni trigonal prisms. This result is quite different from the one previously obtained for a-$Mo_{70}B_{30}$ (Ref. 4) where axial symmetry of the B environment was observed as in c-Mo_2B

(tetragonal I_4/mcm as Ni_2B) (Fig. 12). It is worth noticing that the EFG in a-$Mo_{70}B_{30}$ $(\bar{v}_Q = 420 \pm 40$ kHz) (Ref. 9) is close to (even slightly lower than) that in c-Mo_2B $(\bar{v}_Q = 480 \pm 20$ kHz) in contrast with the case of NiB system; this is consistent with the higher symmetry which certainly implies a longer coherence length of the local structure and hence a smaller difference of V_{zz} in the crystal and in the glass. Such a difference between the structures of $Mo_{70}B_{30}$ and $Ni_{67}B_{33}$ glasses might be related to the fact that Mo_2B is the only stable molybdenum boride phase in that concentration range.

V. CONCLUSION

This NMR study of the electric field gradient around boron in a-$Ni_{100-x}B_x$ glasses shows that for the eutectic composition $(x \simeq 18.5)$ the boron coordination is rather well defined, i.e., the number, nature, and position of the surrounding atoms fluctuate from site to site much less than in a random packed network. Furthermore the symmetry of the boron environment is the same as in c-Ni_3B. It is then concluded that boron is surrounded by nickel trigonal prisms as in most nickel borides, excluding Ni_2B. When boron concentration increases, the degree of fluctuations or the variety of B environment increases as revealed by a broader distribution of the EFG. This variety, however, differs from that expected from random packing since environments with strong asymmetry are absent. Indeed for the highest available boron concentration $(x = 40)$, our results can be quite satisfactorily interpreted if boron environments are trigonal prisms similar to those in c-Ni_4B_3. No axial symmetry corresponding to nickel anticubes as in c-Ni_2B is observed in the glasses but rather there is a continuous variation of the average EFG strength and symmetry with varying B content. It is also suggested that in all glassy nickel borides B is surrounded by 6 Ni atoms arranged on trigonal prisms randomly packed as suggested by Gaskell.[10] To accommodate the increasing boron concentration these prisms would share more Ni atoms with other prisms, ultimately sharing rectangular faces allowing B-B contacts in the high-boron-concentration region.

ACKNOWLEDGMENT

*On leave from the Central Research Institute for Physics, P.O. Box 49, H-1525 Budapest, Hungary.

[1]G. Czjzek, Nucl. Instrum. Methods 199, 37 (1982); G. Czjzek, J. Fink, F. Götz, H. Schmidt, J. M. D. Coey, J. P. Rebouillat, and A. Liénard, Phys. Rev. B 23, 2513 (1981).

[2]P. J. Bray, F. Bucholtz, A. E. Geissberger, and I. A. Harris, Nucl. Instrum. Methods 199, 1 (1982).

[3]P. C. Taylor, E. J. Friedele, and M. Rubinstein, in *Physics of Structurally Disordered Solids*, edited by S. S. Mitra (Plenum, New York, 1974), p. 665.

[4]P. Panissod, D. Aliaga Guerra, A. Amamou, J. Durand, W. L. Johnson, W. L. Carter, and S. J. Poon, Phys. Rev. Lett. 44, 1465 (1980).

[5]I. W. Donald and H. A. Davies, J. Mater. Sci. 15, 2754 (1980).

[6]L. Takacs (private communication).

[7]I. Bakonyi, P. Panissod, and R. Hasegawa, J. Appl. Phys. <u>53</u>, 7771 (1982).

[8]F. A. Kuhnast, Thesis, Nancy, 1979 (unpublished); and Y. N. Petrov, V. V. Kovalev, and M. M. Markus, Dokl. Akad. Nauk SSSR <u>198</u>, 118 (1971).

[9]In Ref. 4, the scale on Fig. 2 is 200 G instead of 100 G. Owing to this scaling error, values for $\bar{\nu}_Q$ in c-Mo_2B, a-$Mo_{70}B_{30}$, and a-$Mo_{42}Ru_{38}B_{20}$ stated in Table I are half the actual ones.

[10]P. H. Gaskell, J. Non-Cryst. Solids <u>32</u>, 207 (1979).

[11]Experimental spectra have been made symmetric in order to improve the signal-to-noise ratio and the accuracy of the determination of the EFG parameters